M.S. THESIS

High Current Operation and Analysis on InGaN/GaN-based LED with Improved Hole Injection Structure

광출력 향상 구조를 적용한 질화갈륨 발광다이오드의 고전류 동작과 분석

BY

SUNGJOON KIM

February 2017

DEPARTMENT OF ELECTRICAL AND
COMPUTER ENGINEERING
COLLEGE OF ENGINEERING
SEOUL NATIONAL UNIVERSITY

ABSTRACT

Advanced light-emitting diodes (LED) with an improved hole injection and straightforward fabrication process and structure are proposed. To confirm the enhancement of hole injection, proposed p-type GaN direct-hole injection plug (DHIP) is closely investigated by numerous simulation results considering size and formation of DHIP. Moreover, the structure is analyzed in hole concentration and radiative recombination in each quantum wells. In the simulation, DHIP LED feature higher light output power about 11% than REF LED. Based on simulation results, The DHIP and REF LED were fabricated on c-plane sapphire substrate. The DHIP is formed on the locally etched multiple-quantum well (MQW) by epitaxial lateral overgrowth (ELO) method. It is confirmed that the light output power is greatly increased up to 23.2% at an operating current density of 100 A/cm^2. Furthermore, in order to identify the origin of optical performance improvement, the transient electroluminescence (EL) decay and light intensity distribution characteristics

were analyzed on the DHIP LED devices. Through calculation and fitting of the EL decay characteristics, internal quantum efficiency (IQE) is precisely extracted along with the recombination coefficients, which reveals that the DHIP has the significant effect on enhancing efficiency droop.

Keywords: Light-emitting diodes (LEDs), hole injection, efficiency droop, internal quantum efficiency (IQE), lateral overgrowth (ELO)

Student number: 2015-20900

CONTENTS

1. Introduction

The nitride-based light-emitting diodes (LEDs) have been widely used for various optical applications thanks to rapid improvements in epitaxial and novel structuring techniques. Especially, the active efforts to enhance electrical/optical conversion efficiency and product lifetime have made LED popular in the large scale ranging from a little toy up to the automotive lamp and city lighting where cost-effective and energy-efficient light sources are of paramount importance.

In recent years, needs on high driving current LED are growing with increasing demands on high brightness lighting products [1, 2]. However, in order to operate the LED at high driving current, the chronic issue of efficiency droop should be solved. The efficiency droop is closely linked with nitride-based material properties [3-6]. The main causes underlying efficiency droop are known to include quantum confinement stark effect (QCSE) by

piezo-electric field, Auger recombination, indium composition fluctuation, and different carrier distribution in quantum wells. When the number of holes delivered from electrode to a quantum well (QW) is insufficiently small, radiative recombination occurs near the p-GaN side QW, which leads to electron overflow from the QW and efficiency lowering [7-11]. In order to improve the efficiency droop, multiple-quantum well (MQW) structures are employed in the recent LED devices through consecutive epitaxial processes [3]. However, although the MQW structure improves the efficiency by resisting the droop to some extent, the effect is not yet clear when the operation needs high driving current for increased brightness.

Numerous researches have been focusing their efforts to make a breakthrough out of this problem. For instance, the strain relaxation and hole injection improvement through forming step-stage relief layer, superlattice structure, V-pits around threading dislocations (TDs), and nanostructure of InGaN/GaN MQW are the widely studied approaches [12-20]. However, in constructing the nanostructures, there can be issues about uniform patterning

over the entire wafer due to inevitable curvatures by lattice mismatch and the difference in thermal expansion coefficients between the epitaxial layers and the substrate, or even among the epitaxial layers. Also, it requires a high cost for the fabrication process.

In this thesis, p-type direct hole injection plug (DHIP) structure is proposed which has higher immunity to the efficiency droop based on simple and cost-effective fabrication architecture. The optimization of DHIP LED is closely investigated by numerous simulation and measurement results from fabricated DHIP LED considering the DHIP size and arrangement.

2. DHIP structure concept and simulation

2.1. DHIP structure concept

The conventional LED structure suffers from insufficient hole injection because of high activation energy and heavy effective mass of Mg acceptors. As shown in Fig. 2.1 and Fig. 2.2, hole concentration in MQW is lowered as closer to n-GaN. And radiative recombination is also gradually decreased. This insufficient hole injection into MQW suppresses the radiative recombination and generates the efficiency droop. To reduce the efficiency droop in conventional MQW LED, various research has proceeded recently. Especially by nanostructuring of MQW, the epitaxial strain on each quantum well could be relaxed. Hole injection is also increased by regrowth the p-GaN or p-AlGaN on nano-patterned MQW. However, it has disadvantages on the aspect of fabrication and leakage current by p-GaN direct contact on n-GaN.

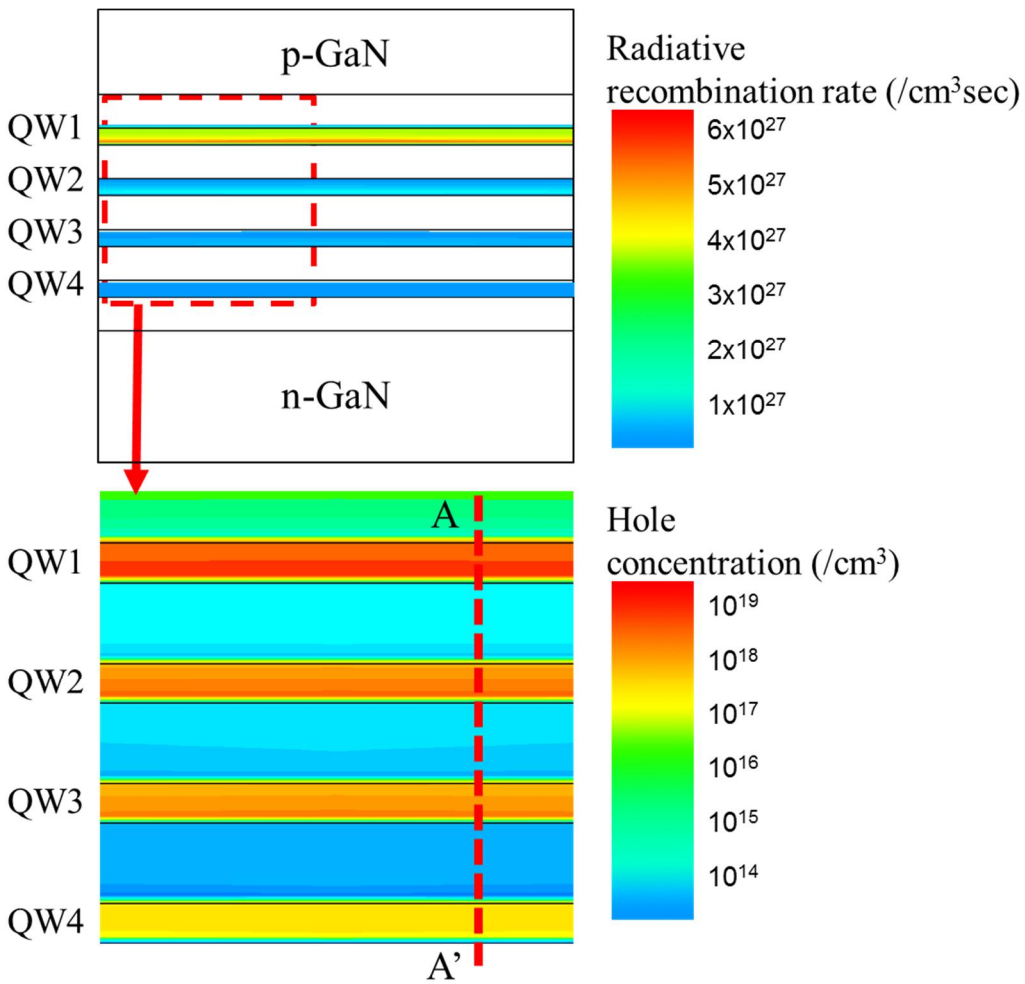

Fig. 2.1 Radiative recombination rate and hole concentration contour image of conventional MQW LED.

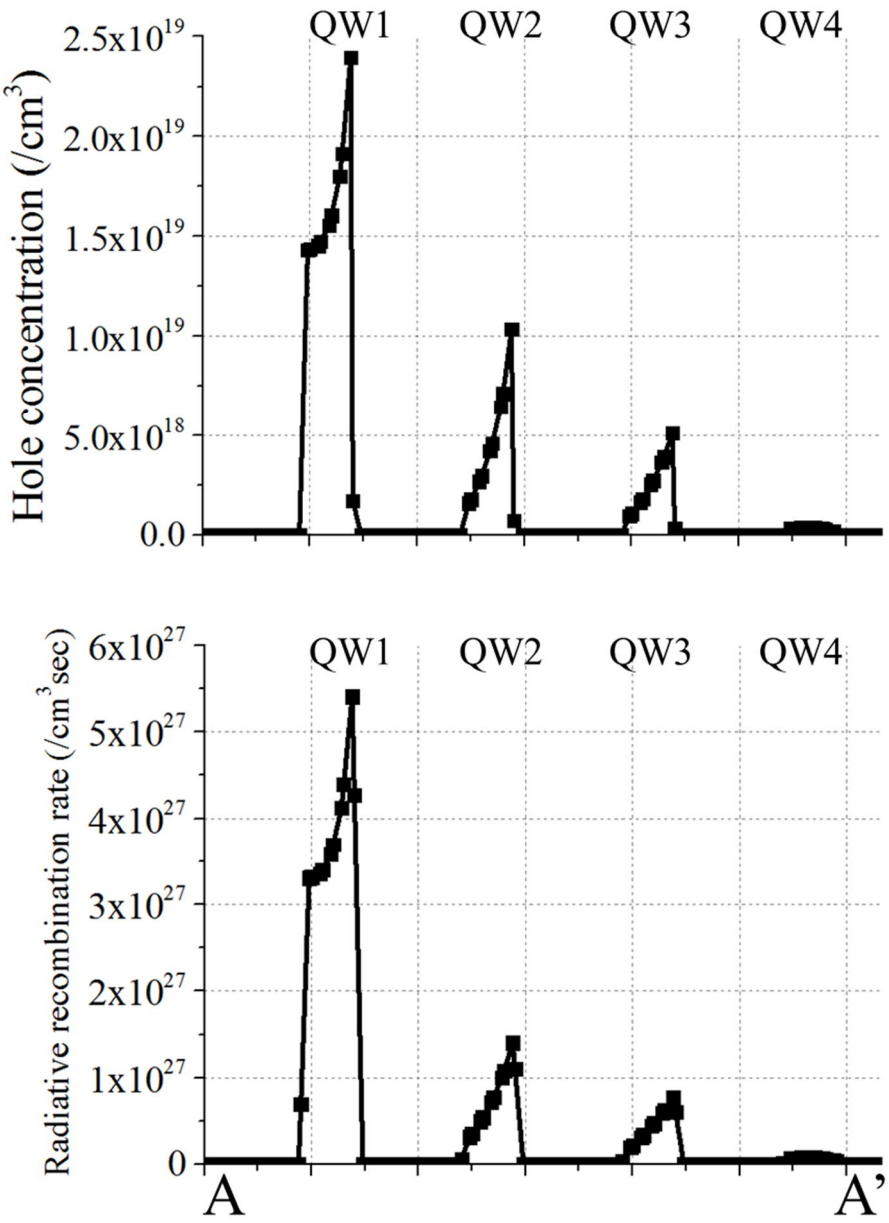

Fig. 2.2 Numerical graph of A-A' region in Fig. 2.1.

Therefore, in this research, direct hole injection plug (DHIP) structure on MQW by straightforward fabrication process with stable operation at low and high current condition is proposed. Fig. 2.3 shows a cross-sectional view of proposed DHIP structure. DHIPs are formed on partly etched MQW by epitaxial lateral overgrowth (ELO) method [21, 22]. By etching the part of 1st QW and regrowth the p-GaN, holes are injected directly into 2nd QW and side direction of 1st QW. It is expected that the DHIP distribute holes to 1st and 2nd and additionally inject into lateral side QWs. Thus, total hole concentration in MQW is expected to increase by DHIP structure.

Table 2.1 Recombination coefficients for simulation.

Recombination coefficients	values
SRH recombination coefficient A (s^{-1})	3.0×10^{6}
Radiative recombination coefficient B (cm^3s^{-1})	2.0×10^{-11}
Auger recombination coefficient C (cm^6s^{-1})	2.0×10^{-31}

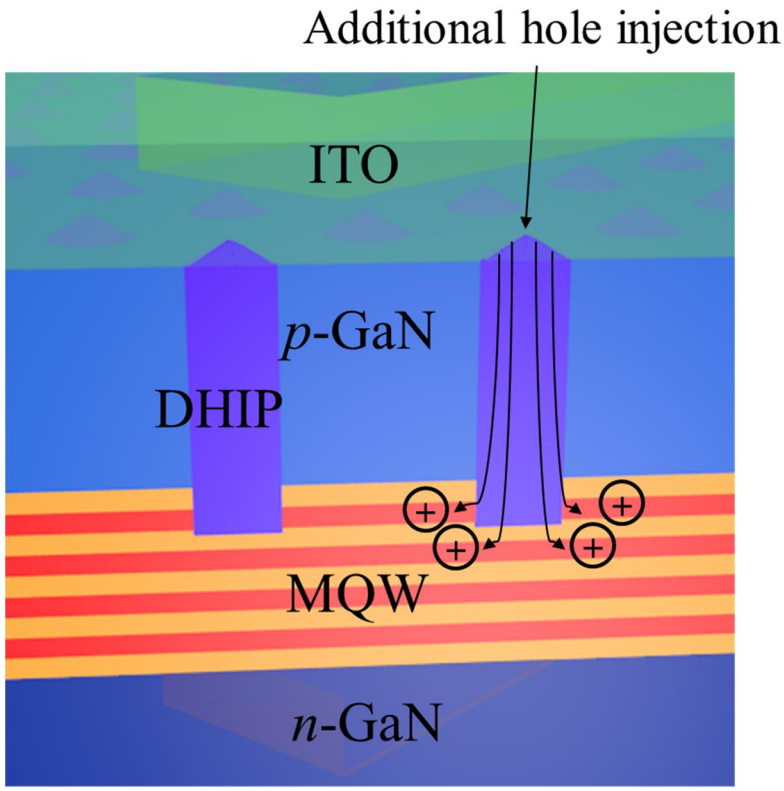

Fig. 2.3 Cross-section image of DHIP structure shows the additional hole injection mechanism.

2.2. Simulation results

The DHIP structure is analyzed by Silvaco 3D TCAD simulation tool. To optimize the DHIP structure, hole concentration and light output power are investigated by varying DHIP depth and width. Fig. 2.4(a) shows a cross section view of simulated DHIP 3D structure. The radius of the active region is 2 μm and DHIP width is varied 0.2 μm to 1.6 μm. To activate 2^{nd} QW, DHIP depth is formed on 2^{nd} QW barrier.

The simulation model includes Fermi statistics, strain, spontaneous recombination, 50% of built-in polarization, 60:40 of GaN/InGaN band offset ($\Delta Ec : \Delta Ev$) ratio, Shockley-Read-Hall (SRH) recombination and Auger recombination. SRH (*A*), radiative (*B*), Auger (*C*) coefficient are constant as shown in Table. 2.1. Overall epitaxial layers consist of n-GaN (thickness: 0.5 μm, doping concentration: n-type 4 x 10^{18} cm^{-3}), four pairs of MQW (GaN/InGaN, 6 nm/3 nm), and p-GaN (thickness: 110 nm, doping concentration: p-type 2 x 10^{19} cm^{-3}). In the Fig. 2.4(b), DHIP structure shows

high hole concentration in 2nd QW as much as 1st QW. Thus, holes are effectively injected into QWs by DHIP on 2nd QW.

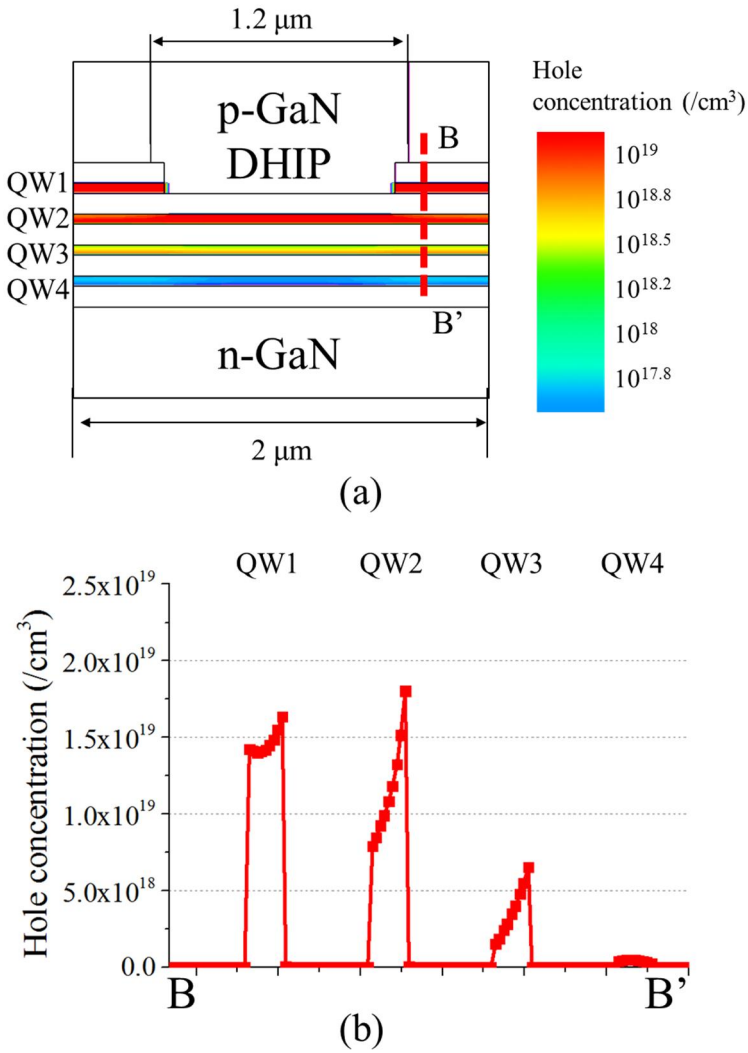

Fig. 2.4 Hole concentration in DHIP structure. (a) Contour image. (b) Numerical hole concentration of each QW in B-B' region.

In the QW under DHIP (2^{nd} QW), the hole concentration and radiative recombination are increased simultaneously. Although the hole concentration in the 1^{st} QW is decreased, total hole concentration is increased because of distributed hole injection at the MQW (Fig. 2.5(a)). Therefore, the light output power is improved by increasing total hole concentration and radiative recombination up to 11% at 100 A/cm^2 (Fig. 2.5(b)).

To optimize the DHIP structure, additional simulations are conducted varying its radius and depth. Increasing radius and depth reduces total hole concentration due to the loss of absolute active area (Fig. 2.6(a)). However, Fig. 2.6(b) shows that the light output power is improved when DHIP is formed deeper (as close to n-GaN). Because the strain is accumulated by stacking QWs, so carrier separation is lowered in QW near n-GaN. Therefore, in the case of DHIP formed on 4^{th} QW, light output power is enhanced steeply in spite of decreased hole concentration. On the other hand, when fabricate the DHIP LED, effect of substrate and buffer layer strain to MQW cannot be known exactly and dry etching damage and regrowth defect around DHIP have

to be considered. By these reasons, the light output power of fabricated DHIP on 4^{th} QW device is expected to lower than simulated results. Considering fabrication challenges, simulated DHIP structure have to increase the total hole concentration and light output power simultaneously. Thus, DHIP on 2^{nd} QW structure is determined to fabricate DHIP LED devices because it satisfies all conditions for enhancing LED performance and minimize the fabrication risks.

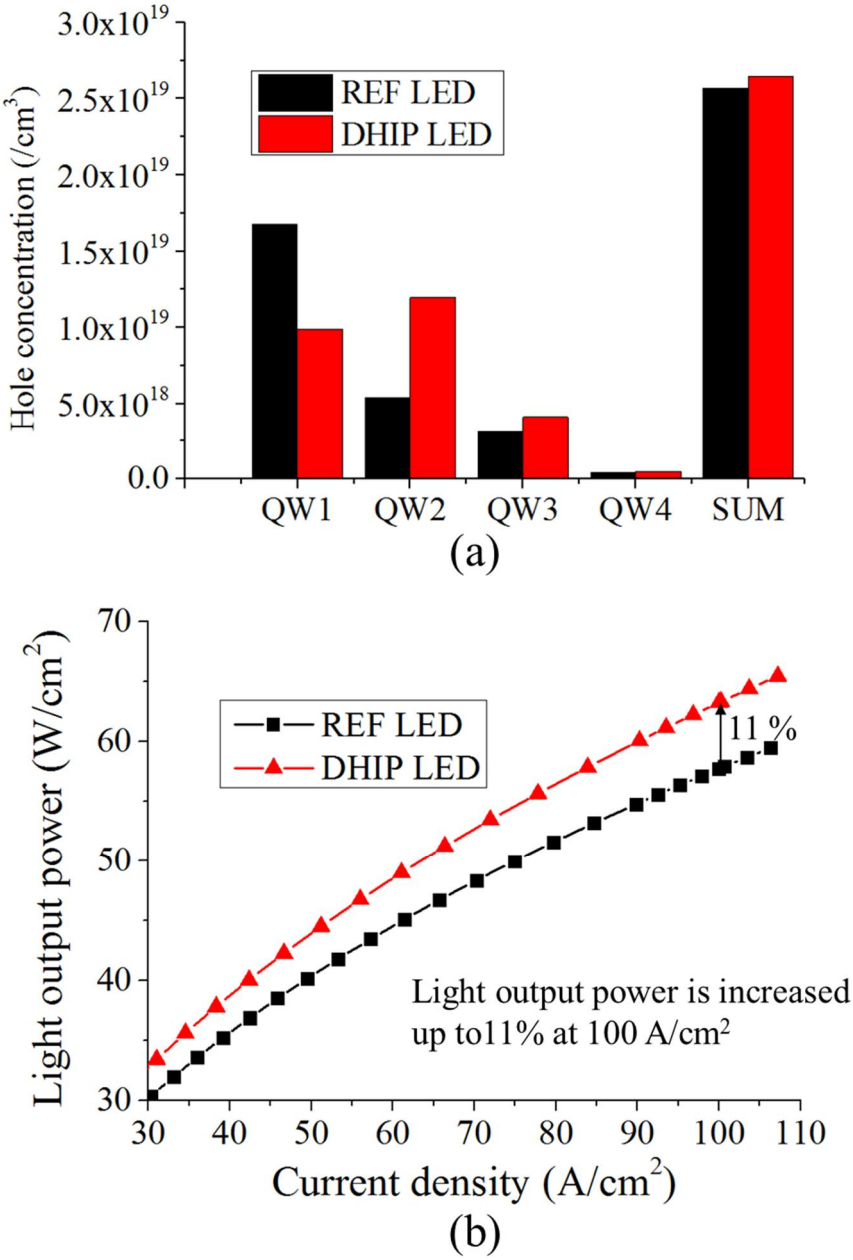

Fig 2.5 (a) The hole concentration in MQW on REF and DHIP LED. (b) A comparison of the light output power between REF and DHIP LED.

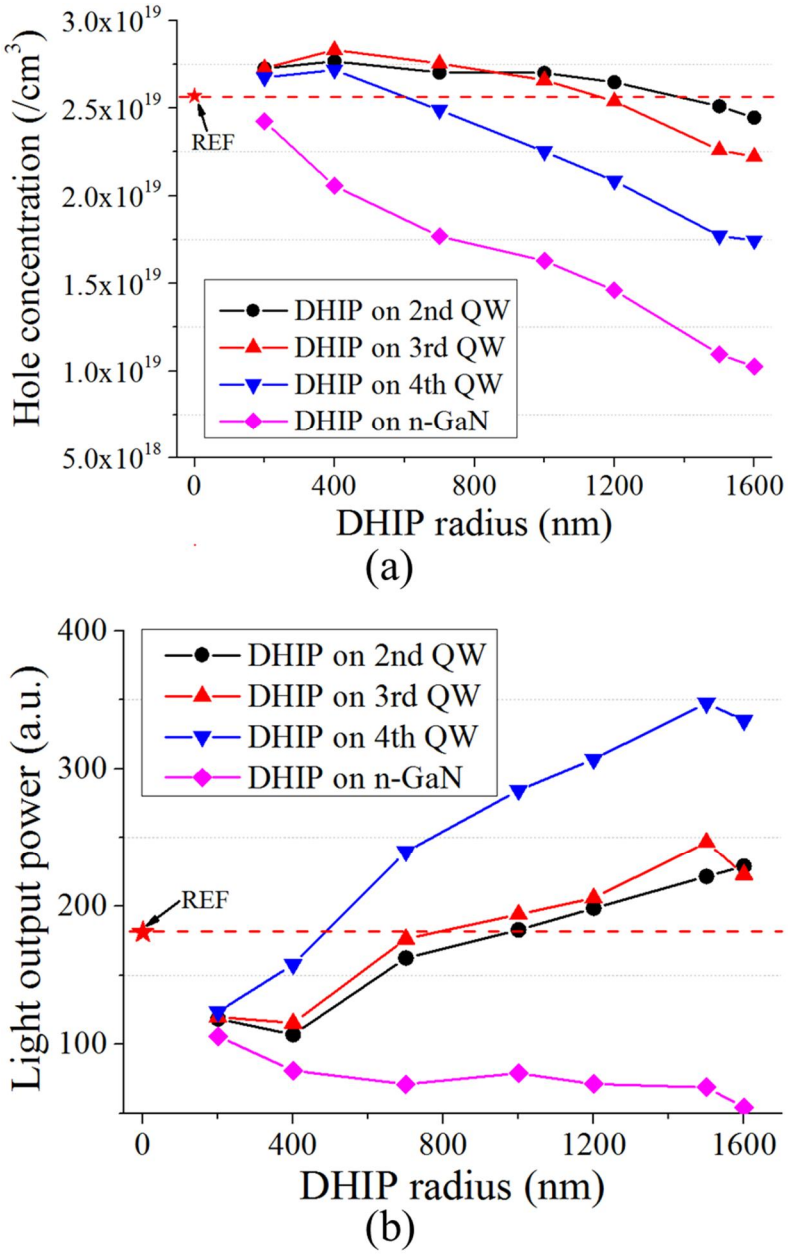

Fig 2.6 DHIP characteristics by varying DHIP radius and depth. (a) The total hole concentration and (b) light output power on MQW vs. DHIP radius.

3. DHIP LED fabrication

3.1. Fabrication process

Fig. 3.1 shows the fabrication process of the suggested p-type GaN DHIP structure. An LED epitaxy is prepared on the 2-inch c-plane sapphire wafer and its peak wavelength is targeted at 445 nm. Here, an MQW has four pairs of InGaN/GaN (3 nm/12 nm). In order to selectively fill the p-GaN on etched MQW, SiO_2 mask (thickness = 200 nm) is deposited on the p-GaN. Then, DHIP split patterning is conducted by photolithography (Table. 3.1). Next, dry etches of the SiO_2 layer and the MQW are carried out to make holes where the DHIPs are regrown. An etch rate of epitaxy is determined to 5.384 nm/sec as shown in Fig 3.2. Here, three QWs remain intact during the dry etch of MQW in order to prevent active region loss and excessive overflow of carriers leading to leakage current at high operating current. After forming the holes on the MQW, holes are selectively filled by p-GaN epitaxial regrowth.

Then, the SiO_2 mask is removed by buffered HF (BHF) solution. After construction of the DHIPs, fabrication of LED devices is proceeded by the lateral LED fabrication process. The active area of a device is 440 μm x 370 μm and indium tin oxide (ITO) transparent p-electrode metal is deposited on all the active regions except the mesa-etched n-GaN regions. Therefore, the ITO layer operates as p-electrode governing the p-GaN and the DHIP together.

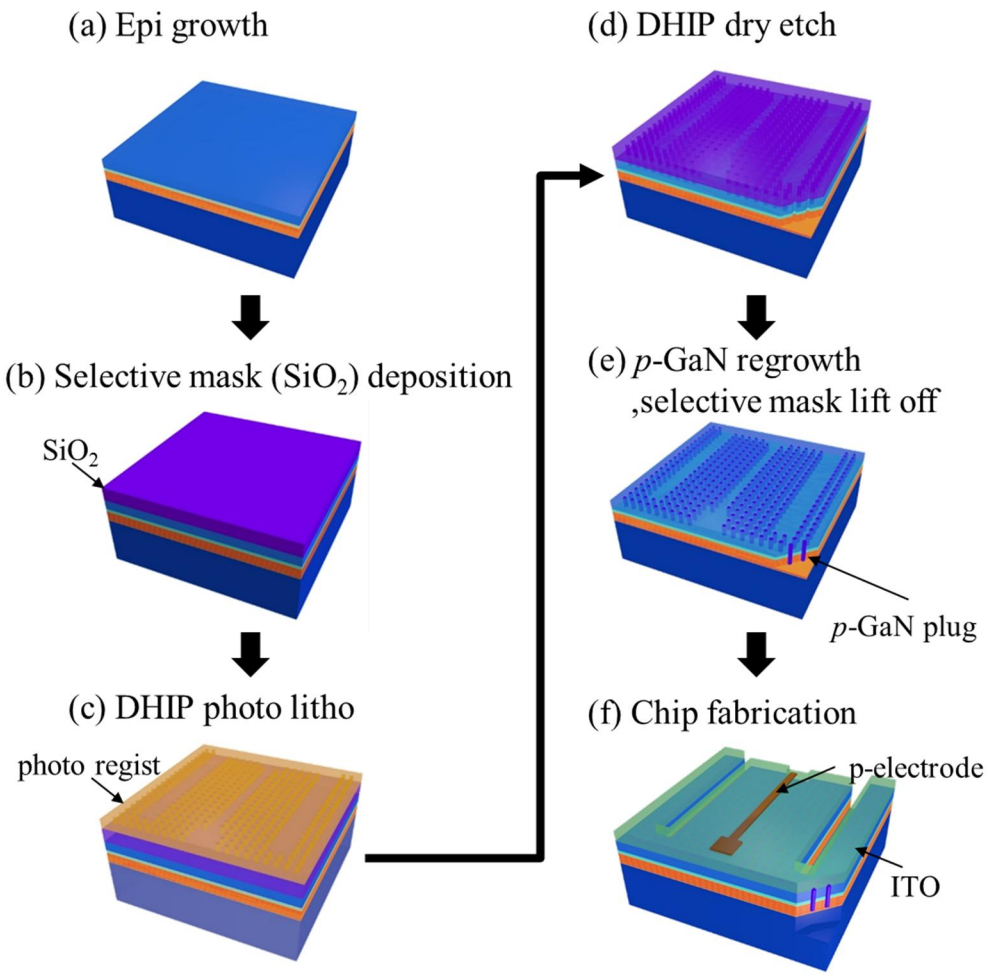

Fig. 3.1 Fabrication process of DHIP LED. (a) Epitaxial growth on the sapphire substrate. (b) Selective growth mask (SiO_2) deposition. (c) DHIP patterning by photolithography. (d) DHIP holes formation using an ICP-RIE dry etch. (e) p-GaN selective regrowth and selective mask lift-off (BHF solution). (f) Lateral type LED device fabrication with ITO transparent metal.

Table 3.1 Photo mask split table by total number and circumference of the DHIPs

	Total DHIP number (ea)				Total DHIP circumference (mm)			
Pitch (μm)	Radius 2 μm	Radius 2.5 μm	Radius 3 μm	Radius 3.5 μm	Radius 2 μm	Radius 2.5 μm	Radius 3 μm	Radius 3.5 μm
6	4,680	3,162			293.9	248.2		
7	3,205		2,300		201.3		216.7	
8	2,348	1,787		1,729	147.5	140.3		190.0
9	1,829				114.9			
10	1,402		1,106		88.1		104.2	
11	947	927		909	59.5	72.8		99.9
13	669		664		42.0		62.6	
16		430		427		33.8		146.9
18	359				22.5			
19			292				27.5	
22				232				25.5

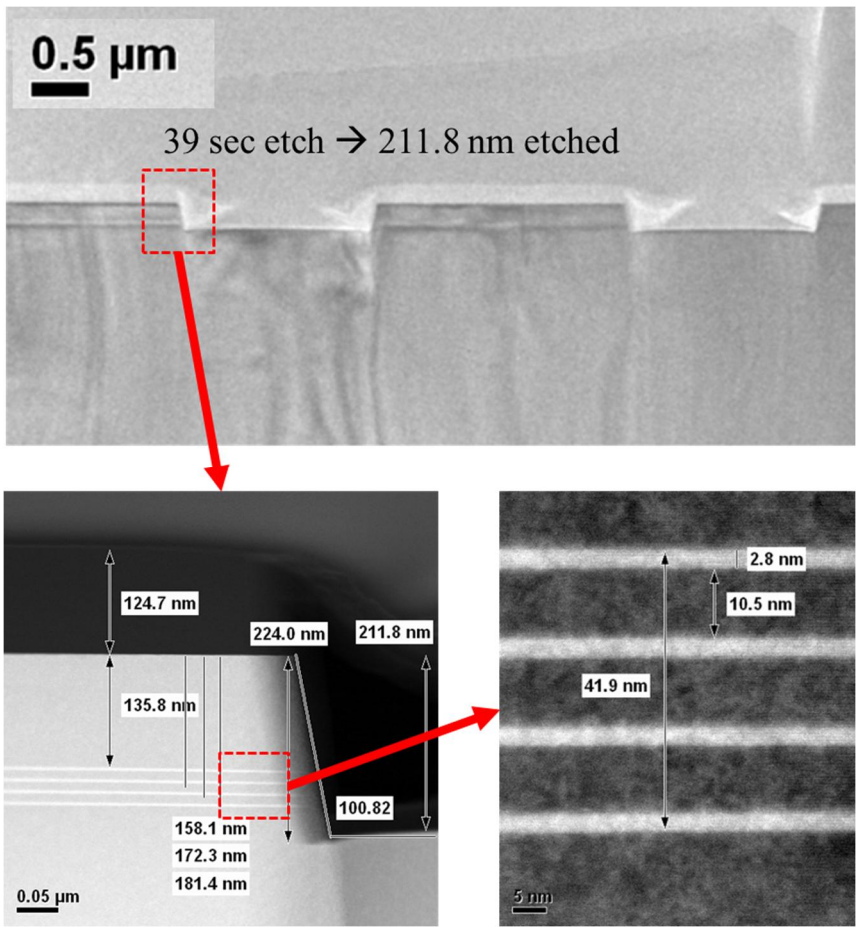

Fig 3.2 TEM image of MQW to examine real thickness of epitaxial layers and dry etch test for etch rate determination.

3.2. Device structure configuration

In order to confirm the structural formation of DHIP, the regrown structure was closely inspected by a scanning electron microscope (SEM) and a transmission electron microscope (TEM) cooperatively. Fig. 3.3(a) shows the SEM image of MQW partly etched in the depth direction. All the plug holes are filled by the p-GaN epitaxy and hexagonal pyramid islands are formed due to the facet directions as shown in Fig. 3.3(b). In the ELO process, the shape of the regrown pattern is changed by growth temperature and gas pressure [21, 22]. To fill the plug patterns, the same process conditions for growing p-GaN in the early stage were adopted again. The etching is verified to reach the wanted depth as demonstrated in Figs. 3.4(a) and (b). The DHIP is regrown on the 2^{nd} QW and completely filled with p-GaN without any void. Through this precisely depth-controlled p-GaN contact on the 2^{nd} QW, increased amount of hole injection is made possible from the DHIP edge to the 1^{st} and the 2^{nd} QW sides as schematically shown in Fig. 2.3. From the

measurement data, the correlations between the total number of plugs and circumference versus optical output power can be quantitatively analyzed.

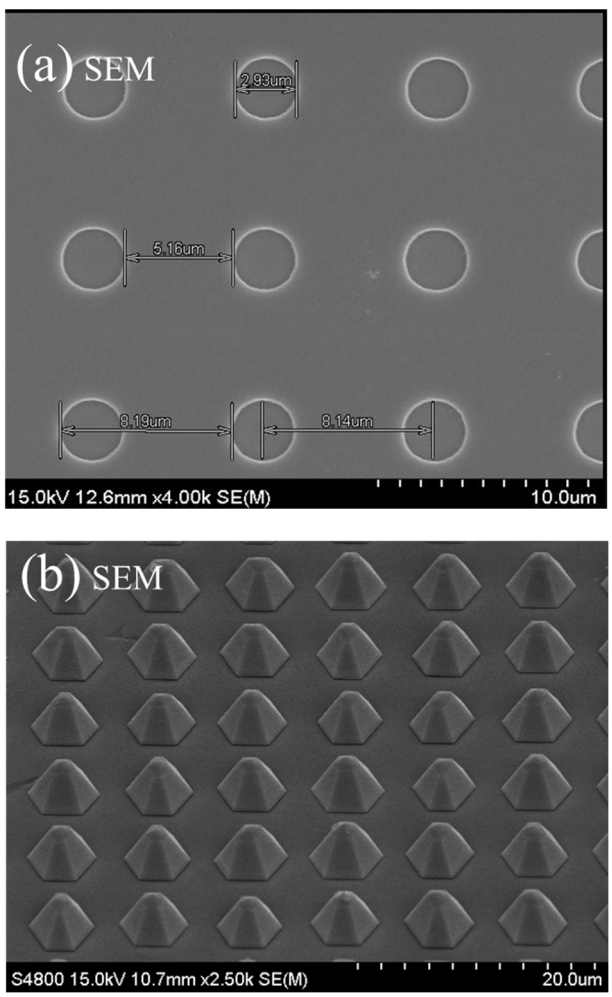

Fig. 3.3 SEM image of (a) etched DHIP region and (b) regrown hexagonal island p-GaN image.

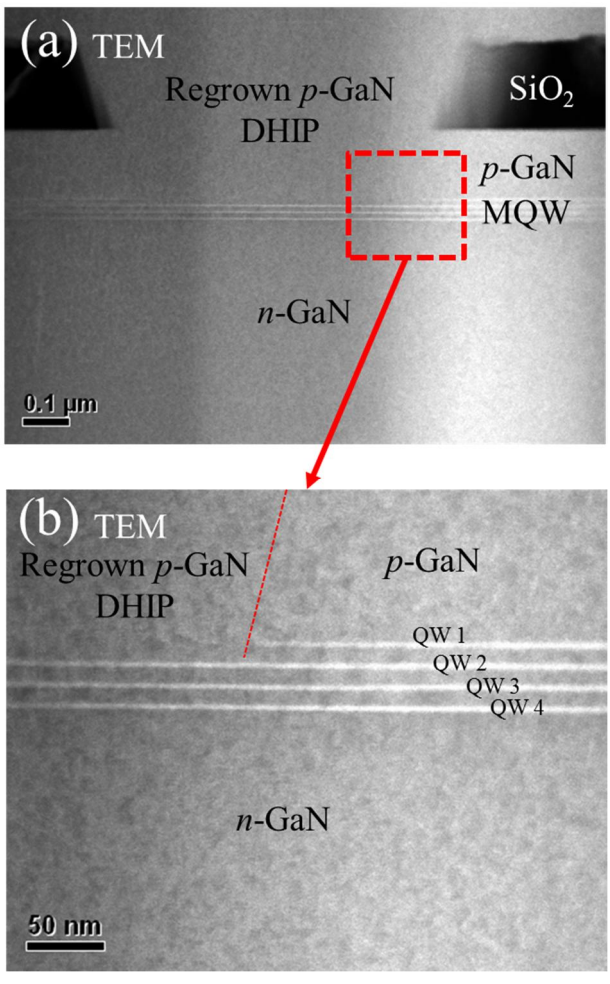

Fig. 3.4 TEM image of (a) cross-sectional DHIP region and (b) enlarged image of Fig 3.4 (a), DHIP successfully formed on 2nd QW.

4. Measurement and analysis on DHIP LED

4.1. PL intensity analysis

After the DHIP fabrication, the mapping photoluminescence (mapping PL) is measured and it is classified clearly to the REF and DHIP LED (Fig. 4.1). PL peak intensity is improved by increasing number of DHIP up to 70%. The intensity improvement is clearly shown in PL spectrum (Fig 4.2).

However, in the PL measurement condition, electron and hole are not directly injected to MQW. So, it is expected that there is another reason for increase PL intensity except for additional hole injection mechanism. And the clue is easily found in the structural shape of DHIP pattern. When DHIP growing in the etched region, the epitaxy is formed as the hexagonal pyramid shape. The size of DHIP etch and regrowth pattern is measured as 3 um and 6.8 um respectively. Due to the epitaxial growth condition (temperature, pressure) affects the regrowth shape, it is possible that modify the hexagonal

pyramid width and height. The critical angle to extract the light become larger by form the hexagonal pyramid pattern. Therefore, the extraction efficiency is also increased by DHIP regrowth structure.

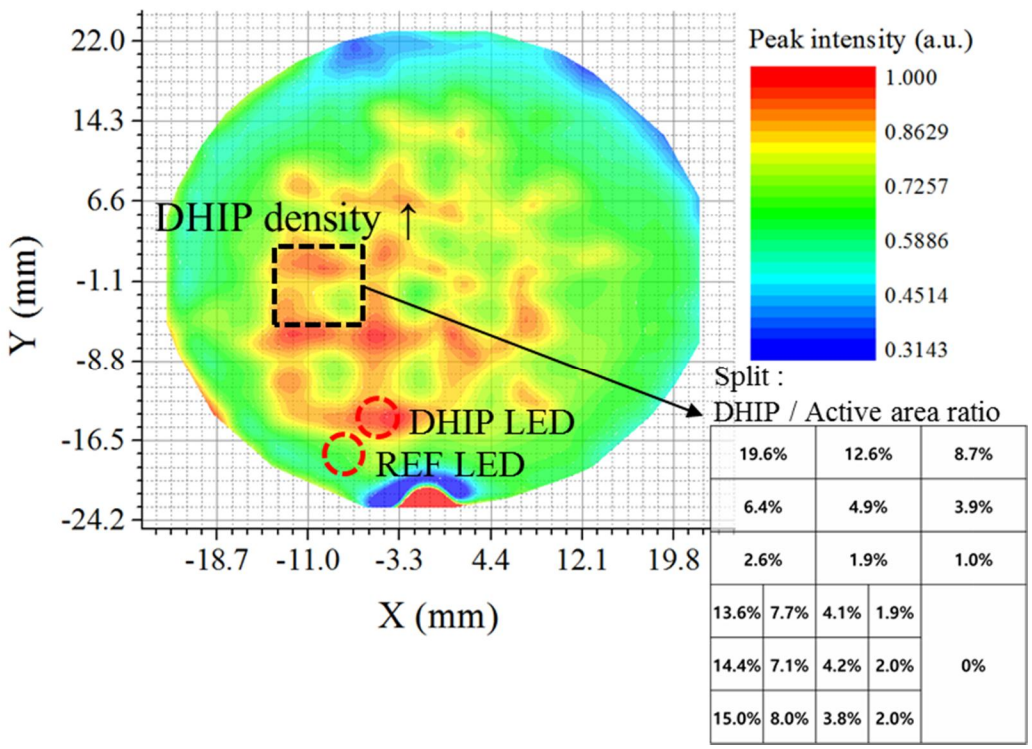

Fig. 4.1 Mapping PL result on whole wafer area, PL intensity is enhanced by increasing number of DHIP.

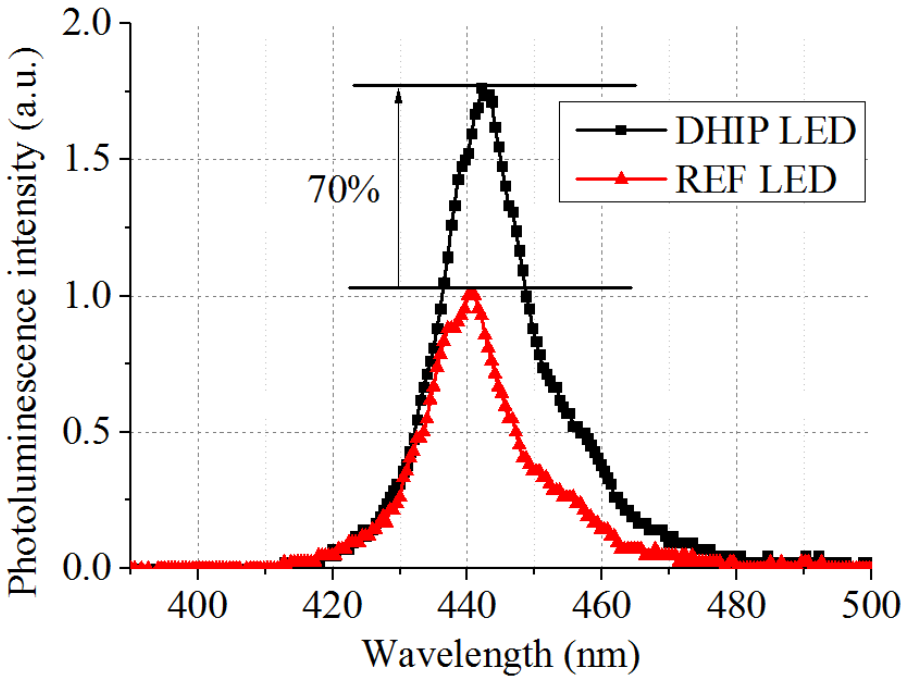

Fig. 4.2 PL spectrum comparison between REF and DHIP LED, peak PL intensity is increased up to 70%.

4.2. LI curve and EL intensity distribution

The DHIP and REF LED went through the same fabrication process, in the same critical dimensions, with the DHIP LEDs but REF LED has no DHIP structures. Further, in order to study the effect of the number of DHIPs, DHIP LED devices having different numbers of DHIPs were fabricated at the same time, where the DHIPs have the same radius of 3 μm. Thus, the final independent variable is the circumference of all the DHIPs and its effects on optical performances are investigated. Fig. 4.3(a) shows the light output power as a function of current density. The light output power shows a steeper increase in the DHIP LED than in the REF LED. The difference in light output power becomes more noticeable in the high current region above 35 A/cm^2. Compared with the DHIP LED with total 1,106 plugs, the DHIP LED having less plugs, 664 DHIPs, shows a consistently higher output power. The DHIP LED with 664 DHIPs demonstrates 23.2% increase in light output at 100 A/cm^2. The efficiency droop is also improved phenomenally as shown in Fig.

4.3(b).

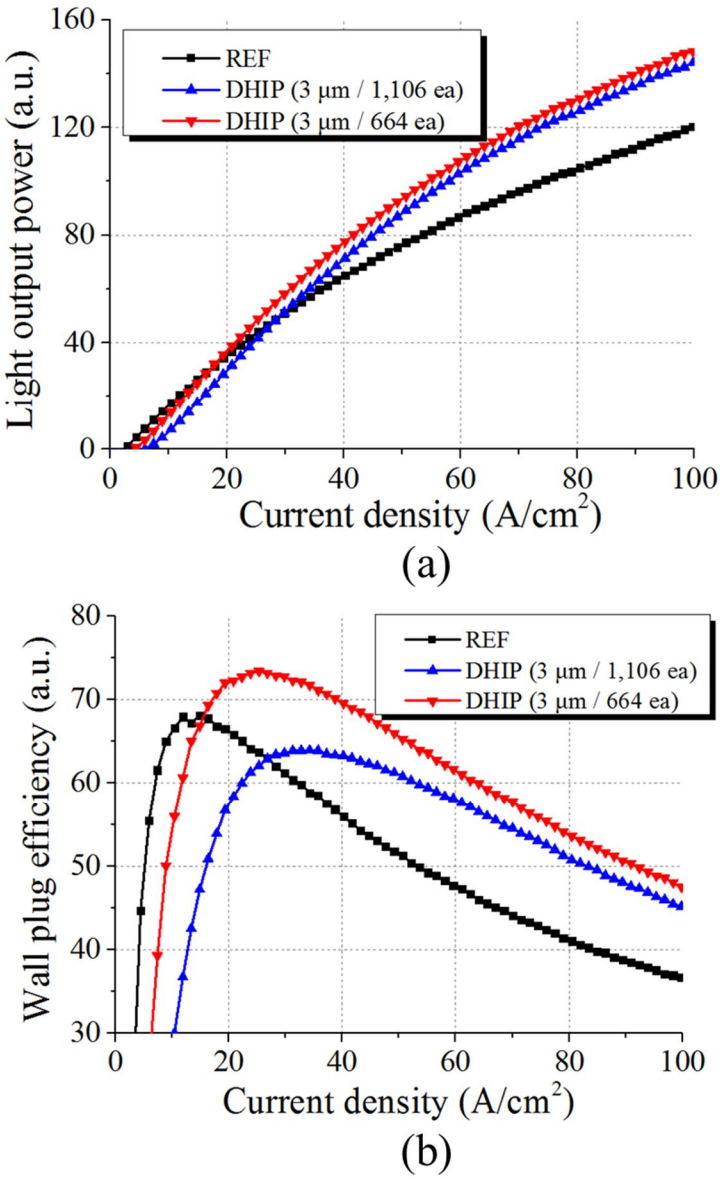

Fig. 4.3 Comparison of optical performances among the fabricated devices. (a) Measured light output power vs. current density. (b) Wall plug efficiency vs.

current density.

In order to confirm that the enhancement of light output power actually comes from the DHIPs, electroluminescence (EL) intensity distributions were analyzed under different current density conditions. Due to the different tendencies of light output power at low and high current density regimes, the analyses were performed at 4 A/cm^2 and 75 A/cm^2, separately. For a fair comparison, the image capturing options were fixed and all the intensities were normalized in the same scale according to each current density condition. As shown in Figs. 4.4(a) and 4.4(b), the EL intensity of DHIP LED device is lower than that of REF LED at low current injection. However, at high current injection, it is clearly demonstrated by Figs. 4.4(c) and 4.4(d) that the EL intensity over the entire device of DHIP LED is higher than that of REF LED and high-intensity spots are more prominent around the plugs in the DHIP LED device. Also, the current spreading is more effective in the case of DHIP LED due to the distributed hole and electron conduction paths by densely and regularly arranged plugs over the entire active region.

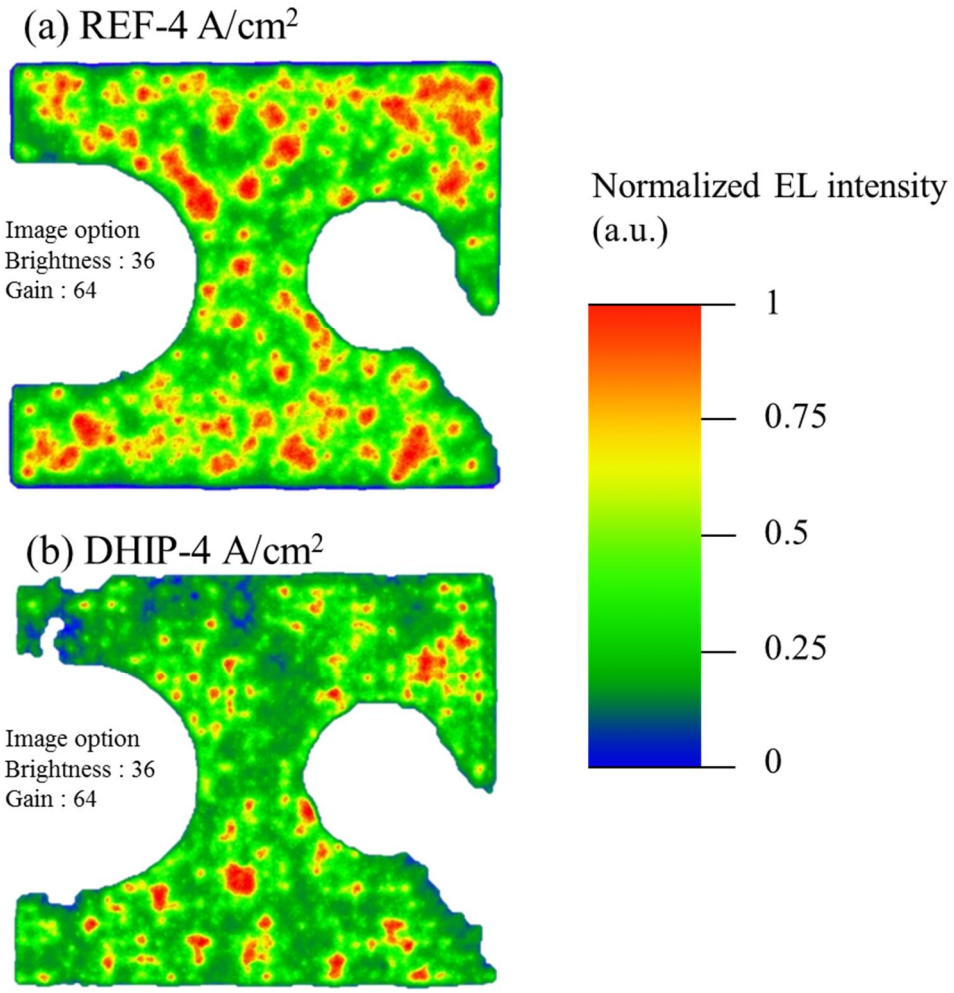
(a) REF-4 A/cm2
Image option
Brightness : 36
Gain : 64
(b) DHIP-4 A/cm2
Image option
Brightness : 36
Gain : 64
Normalized EL intensity
(a.u.)
1
0.75
0.5
0.25
0

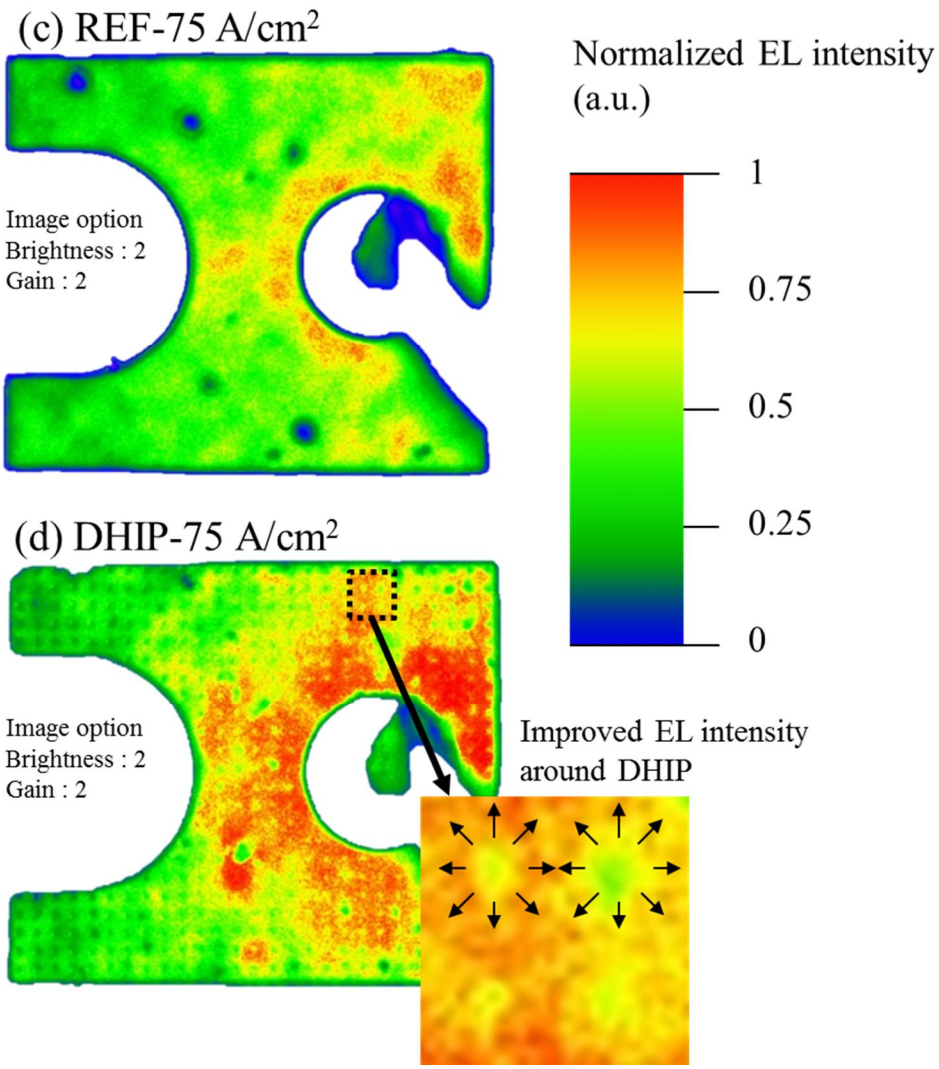

Fig. 4.4 Light intensity distribution images from REF and DHIP LED at current densities of 4 A/cm^2 (a), (b) and 75 A/cm^2 (c), (d) respectively, images were obtained by microscope camera TUCSEN ISH300 and analyzed by the

EtaMax light distinct viewer.

4.3. Extraction of IQE by measuring transient EL decay characteristics

Although it is confirmed that the EL intensity is significantly increased with the help of DHIP structures, there is a slight decrease in the optical power when the total number of DHIPs is increased. In order to perform a quantitative analysis of this unexpected result, *ABC*-model that can accurately discriminate Shockley-Read-Hall (SRH) recombination (*A*), radiative recombination (*B*), and Auger recombination (*C*) coefficients is employed [23-27]. The EL intensity decay characteristics are measured to extract the recombination parameters which can be calculated in the subsequent step by fitting the theoretical decay characteristic to the measured curve (Eq 4.1 to 4.3).

$$-\frac{dn}{dt} = An + Bn^2 + Cn^3 \tag{4.1}$$

$$t = \frac{1}{2A}\left[\frac{2B\tan^{-1}\left(\frac{B+2Cn}{\sqrt{4AC-B^2}}\right)}{\sqrt{4AC-B^2}} + ln\left(A+n(B+Cn)\right) - 2\ln n\right] + t_0 \tag{4.2}$$

$$t_0 = \frac{1}{2A}\left[\frac{2B\tan^{-1}\left(\frac{B+2Cn_0}{\sqrt{4AC-B^2}}\right)}{\sqrt{4AC-B^2}} + ln\left(A+n_0(B+Cn_0)\right) - 2\ln n_0\right] \tag{4.3}$$

The current pulse is applied with an amplitude of 30 A/cm^2 for a duration of 4 μs during a period of 6 μs to characterize EL decay. Equipment setup for measuring EL decay characteristics is shown in Fig. 4.5. Fig. 4.6(a) through 4.6(c) shows the EL decaying of the REF and DHIP LED devices [24].

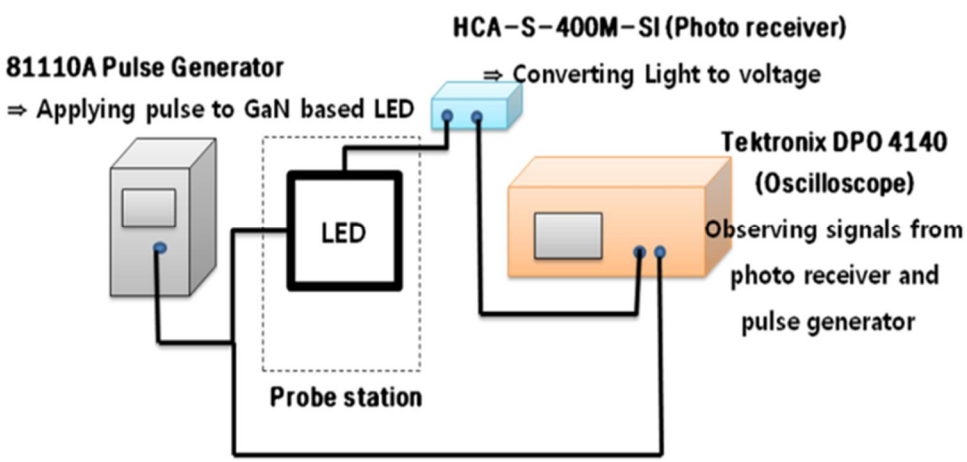

Fig. 4.5 Measurement setup for obtaining EL intensity decay characteristics on REF and DHIP LEDs.

The fitted curves from using the theoretical decay characteristics show good agreements with the measurement results in all cases. As shown in the figures, DHIP LEDs show steeper decay than REF device.

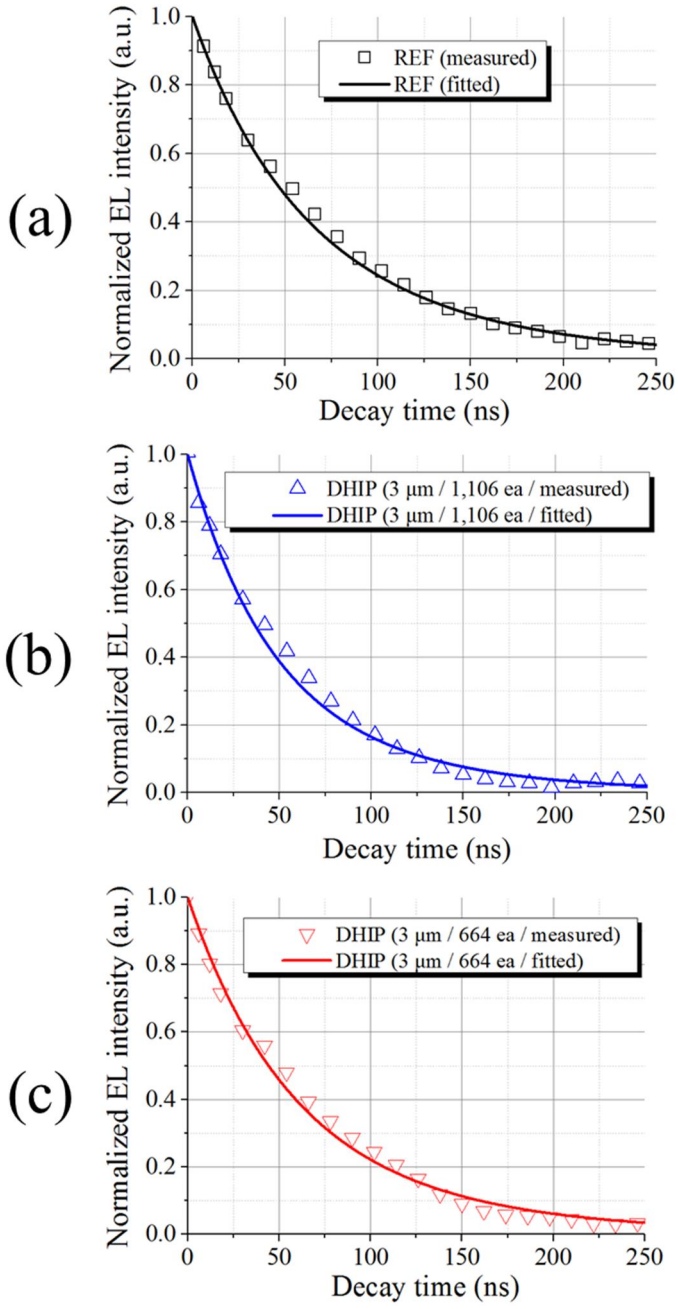

Fig. 4.6 Measured and calculated EL decay curves from (a) REF LED, (b) DHIP LED having radius of 3 μm and total number of 1,106 ea and (c) 664 ea

Table 4.1 Calculated recombination coefficients (*A*, SRH recombination coefficient; *B*, radiative recombination coefficient; *C*, Auger recombination coefficient)

	A (s^{-1})	B (cm^3s^{-1})	C (cm^6s^{-1})
REF	4.7×10^{6}	1.8×10^{-11}	1.5×10^{-31}
DHIP (3 μm / 1,106 ea)	7.6×10^{6}	2.4×10^{-11}	1.5×10^{-31}
DHIP (3 μm / 664 ea)	6.0×10^{6}	2.5×10^{-11}	1.5×10^{-31}

By fitting the theoretical decay characteristics, recombination parameters can be determined as listed in Table 4.1 Among the coefficients, the SRH recombination coefficient increases as the number of DHIPs increases from 664 to 1,106, or equivalently, as the circumference of DHIPs increases from 62.6 mm to 104.2 mm. This result implies that the regrown DHIP regions contain more point defects compared with the intact p-GaN region due to the remaining oxide atoms and plasma damages on the etched GaN surfaces. Also, unwanted Mg diffusion can take place through the side

surfaces of QWs during the p-GaN regrowth process, by which non-radiative recombination can be caused. Consequently, the increased non-radiative recombination centers can lower the radiative recombination probability at low current density. On the other hand, radiative recombination has the predominance and point defects do not significantly affect the efficiency droop at high current density [28].

Radiative recombination coefficient *B*'s of DHIP LEDs are 33% higher than that of REF LED owing to lateral hole injection. Therefore, it is clear that higher *B* values of DHIP LEDs contribute higher EL intensities of the devices than those of REF LED and higher *A* value of DHIP LED with more DHIPs results in its lower EL intensity compared with the device with less DHIPs. The internal quantum efficiency (IQE) is also improved as shown in Fig. 4.7, where the same trend with the wall plug efficiency (WPE) is observed. It is found that DHIP structure significantly improves the optical output power and increases the local defect density in the vicinity of the plugs at the same time. Although the latter effect would not be so apparent in the practical operating

current region, the number of plugs can be optimized for better performance.

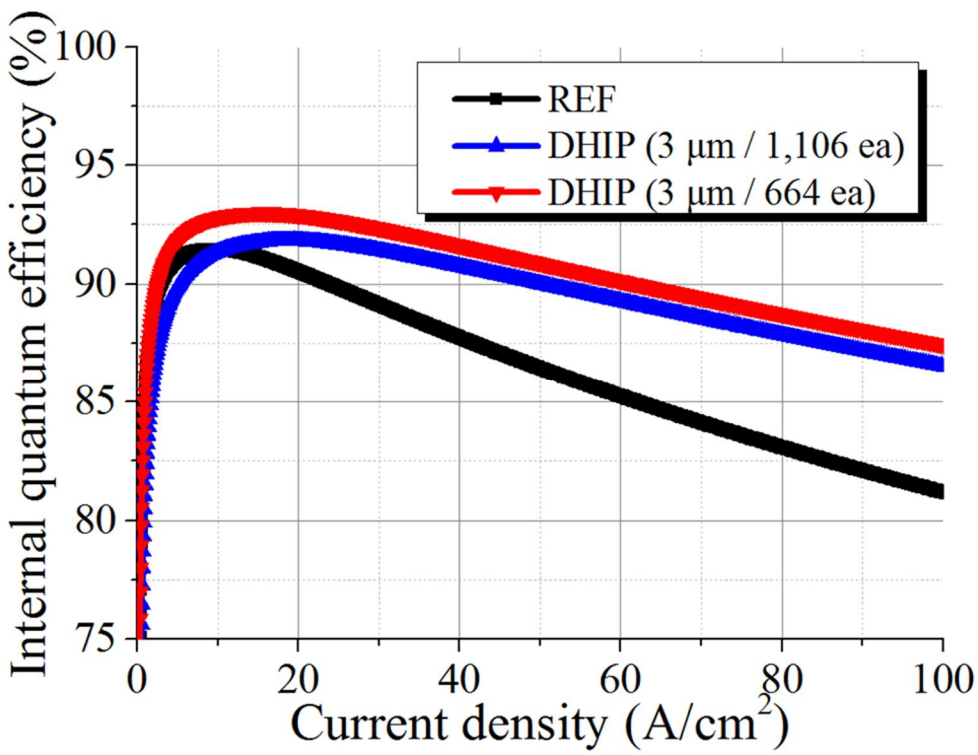

Fig. 4.7 Extracted IQE vs. current density curves of REF and DHIP LEDs obtained from EL intensity decay times

For the optimization task, experiments are expanded to the larger number of DHIP LED devices having a different number of DHIPs with the radius of 2 μm to 3.5 μm to set DHIP circumference as the independent variable in the new analysis. Fig. 4.8(a) demonstrates that the optimal DHIP circumference is located near 75 mm according to the measurement data and the fitting curve. The injection enhancement effect by larger DHIP circumference is dominant up to the optimal point but the non-radiative recombination effect by increased point defects becomes more prominent above the point. In addition, Fig 4.8(b) shows that peak wavelength is shortened by increasing circumference. This result means that the epitaxial strain relaxed at the etched DHIP edge region. Thus, the total number of DHIP should be optimally controlled considering the total plug circumference in practice.

To optimize the low current characteristics on DHIP LED, dry etching damages and point defects should be eliminated. And previous researches

propose some methods for reducing the plasma damage by annealing, wet etch clean by hot KOH, N_2 plasma treatment. [29, 30]

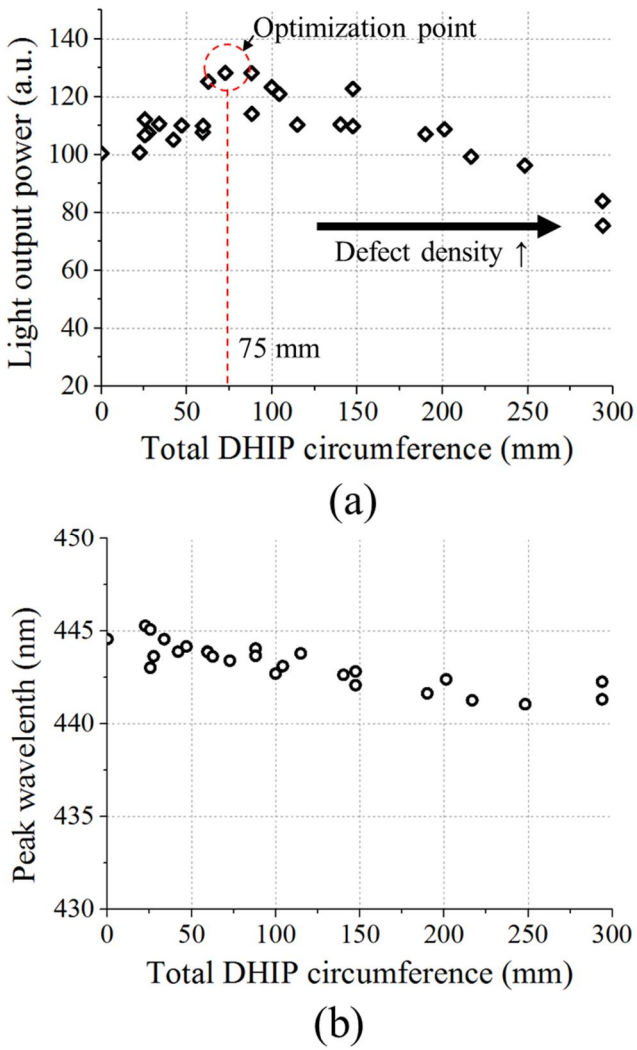

Fig. 4.8 (a) Light output power vs. total DHIP circumference at current density

75 A/cm^2. The location of optimum circumference length near 75 nm is confirmed. (b) Peak wavelength related with the total circumference as the aspect of strain relaxation.

5. Conclusion

In this thesis, p-type GaN DHIP structure has been introduced on the GaN MQW LED for improving the hole injection efficiency, and the straightforward fabrication architecture and the characterization results have been demonstrated. The p-type DHIP is examined by numerous simulation results. The DHIP is analyzed in hole concentration on each QW and features higher total hole concentration and light output power. In the simulation result, DHIP LED feature higher light output power about 11% than REF LED. By measuring the fabricated DHIP LED, it is confirmed that light output power is enhanced up to 23.2% at 100 A/cm^2. In order to analyze the lateral hole injection efficacy in the DHIP LEDs, EL intensity distribution was high-precision mapped and revealed that the increased EL intensity attributes to the DHIPs. Also, the EL characteristics of DHIP LEDs are specifically

investigated by EL decay measurements and parameter extraction for IQE evaluation. According to the calculated IQEs, the density of point defects induced by epitaxial regrowth should be minimized in designing the device structure and the process integration due to its effect of increasing non-radiative recombination under the low-current operating condition. It was found from the expanded experiments that the optimum total DHIP circumference is located around 75 mm.

References

[1] G. Chen, M. Craven, A. Kim, A. Munkholm, S. Watanabe, M. Camras, W. Götz, and F. Steranka, "Performance of high□power III□nitride light emitting diodes," P*hysica status solidi (a),* vol. 205, no. 5, pp. 1086-1092, 2008.

[2] S. Pimputkar, J. S. Speck, S. P. DenBaars, and S. Nakamura, "Prospects for LED lighting," *Nature Photonics,* vol. 3, no. 4, pp. 180-182, 2009.

[3] S. Nakamura, "The roles of structural imperfections in InGaN-based blue light-emitting diodes and laser diodes," *Science,* vol. 281, no. 5379, pp. 956-961, 1998.

[4] J. Piprek, "Efficiency droop in nitride□based light□emitting diodes," *Physica status solidi (a),* vol. 207, no. 10, pp. 2217-2225, 2010.

[5] J. Cho, E. F. Schubert, and J. K. Kim, "Efficiency droop in light□emitting diodes: Challenges and countermeasures," *Laser & Photonics Reviews,* vol. 7, no. 3, pp. 408-421, 2013.

[6] G. Verzellesi, D. Saguatti, M. Meneghini, F. Bertazzi, M. Goano, G. Meneghesso, and E. Zanoni, “Efficiency droop in InGaN/GaN blue light-emitting diodes: Physical mechanisms and remedies,” *Journal of Applied Physics,* vol. 114, no. 7, pp. 071101, 2013.

[7] S. Chichibu, T. Azuhata, T. Sota, and S. Nakamura, “Spontaneous emission of localized excitons in InGaN single and multiquantum well structures,” *Applied Physics Letters,* vol. 69, no. 27, pp. 4188-4190, 1996.

[8] T. Takeuchi, C. Wetzel, S. Yamaguchi, H. Sakai, H. Amano, I. Akasaki, Y. Kaneko, S. Nakagawa, Y. Yamaoka, and N. Yamada, “Determination of piezoelectric fields in strained GaInN quantum wells using the quantum-confined Stark effect,” *Applied physics letters,* vol. 73, no. 12, pp. 1691, 1998.

[9] H. Cho, J. Lee, G. Yang, and C. Kim, “Formation mechanism of V defects in the InGaN/GaN multiple quantum wells grown on GaN layers with low threading dislocation density,” *Applied Physics Letters,*

vol. 79, pp. 215, 2001.

[10] A. David, M. J. Grundmann, J. F. Kaeding, N. F. Gardner, T. G. Mihopoulos, and M. R. Krames, “Carrier distribution in (0001) InGaN/ GaN multiple quantum well light-emitting diodes,” *Applied Physics Letters,* vol. 92, no. 5, pp. 053502, 2008.

[11] D. S. Meyaard, G.-B. Lin, Q. Shan, J. Cho, E. F. Schubert, H. Shim, M.-H. Kim, and C. Sone, “Asymmetry of carrier transport leading to efficiency droop in GaInN based light-emitting diodes,” *Applied Physics Letters,* vol. 99, no. 25, pp. 251115, 2011.

[12] J. Xu, M. F. Schubert, A. N. Noemaun, D. Zhu, J. K. Kim, E. F. Schubert, M. H. Kim, H. J. Chung, S. Yoon, and C. Sone, “Reduction in efficiency droop, forward voltage, ideality factor, and wavelength shift in polarization-matched GaInN/GaInN multi-quantum-well light-emitting diodes,” *Applied Physics Letters,* vol. 94, no. 1, pp. 011113, 2009.

[13] V. Ramesh, A. Kikuchi, K. Kishino, M. Funato, and Y. Kawakami,

"Strain relaxation effect by nanotexturing InGaN/GaN multiple quantum well," *Journal of Applied Physics,* vol. 107, no. 11, pp. 114303, 2010.

[14] J. H. Son, and J.-L. Lee, "Strain engineering for the solution of efficiency droop in InGaN/GaN light-emitting diodes," *Optics Express,* vol. 18, no. 6, pp. 5466-5471, 2010/03/15, 2010.

[15] C. H. Wang, C. C. Ke, C. Y. Lee, S. P. Chang, W. T. Chang, J. C. Li, Z. Y. Li, H. C. Yang, H. C. Kuo, T. C. Lu, and S. C. Wang, "Hole injection and efficiency droop improvement in InGaN/GaN light-emitting diodes by band-engineered electron blocking layer," *Applied Physics Letters,* vol. 97, no. 26, pp. 261103, 2010.

[16] J. Zhu, L. Wang, S. Zhang, H. Wang, D. Zhao, J. Zhu, Z. Liu, D. Jiang, and H. Yang, "Light extraction efficiency improvement and strain relaxation in InGaN/GaN multiple quantum well nanopillars," *Journal of Applied Physics,* vol. 109, no. 8, pp. 084339, 2011.

[17] C. Jia, T. Yu, H. Lu, C. Zhong, Y. Sun, Y. Tong, and G. Zhang,

"Performance improvement of GaN-based LEDs with step stage InGaN/GaN strain relief layers in GaN-based blue LEDs," *Optics express,* vol. 21, no. 7, pp. 8444-8449, 2013.

[18] G. Kim, J. Kim, E. Park, D. Kang, and B.-G. Park, "Improved internal quantum efficiency of GaN-based light emitting diodes using p-AlGaN trench in multi-quantum well," *Japanese Journal of Applied Physics,* vol. 53, no. 6S, pp. 06JE14, 2014.

[19] J. Kim, Y.-H. Cho, D.-S. Ko, X.-S. Li, J.-Y. Won, E. Lee, S.-H. Park, J.-Y. Kim, and S. Kim, "Influence of V-pits on the efficiency droop in InGaN/GaN quantum wells," *Optics express,* vol. 22, no. 103, pp. A857-A866, 2014.

[20] L. Cheng, S. Wu, C. Xia, and H. Chen, "Efficiency droop improvement in InGaN light-emitting diodes with graded InGaN barriers of increasing indium composition," *Journal of Applied Physics,* vol. 118, no. 10, pp. 103103, 2015.

[21] K. Hiramatsu, K. Nishiyama, A. Motogaito, H. Miyake, Y. Iyechika,

and T. Maeda, “Recent Progress in Selective Area Growth and Epitaxial Lateral Overgrowth of III□Nitrides: Effects of Reactor Pressure in MOVPE Growth,” *Physica status solidi (a),* vol. 176, no. 1, pp. 535-543, 1999.

[22] K. Hiramatsu, “Epitaxial lateral overgrowth techniques used in group III nitride epitaxy,” *Journal of Physics: Condensed Matter,* vol. 13, no. 32, pp. 6961, 2001.

[23] P. Kivisaari, L. Riuttanen, J. Oksanen, S. Suihkonen, M. Ali, H. Lipsanen, and J. Tulkki, “Electrical measurement of internal quantum efficiency and extraction efficiency of III-N light-emitting diodes,” *Applied Physics Letters,* vol. 101, no. 2, pp. 021113, 2012.

[24] G. Kim, J. H. Kim, E. H. Park, D. Kang, and B.-G. Park, “Extraction of recombination coefficients and internal quantum efficiency of GaN-based light emitting diodes considering effective volume of active region,” *Optics Express,* vol. 22, no. 2, pp. 1235-1242, 2014/01/27, 2014.

[25] S. Karpov, “ABC-model for interpretation of internal quantum efficiency and its droop in III-nitride LEDs: a review,” *Optical and Quantum Electronics,* vol. 47, no. 6, pp. 1293-1303, 2015.

[26] G.-B. Lin, E. F. Schubert, J. Cho, J. H. Park, and J. K. Kim, “Onset of the Efficiency Droop in GaInN Quantum Well Light-Emitting Diodes under Photoluminescence and Electroluminescence Excitation,” *ACS Photonics,* vol. 2, no. 8, pp. 1013-1018, 2015/08/19, 2015.

[27] X. Meng, L. Wang, Z. Hao, Y. Luo, C. Sun, Y. Han, B. Xiong, J. Wang, and H. Li, “Study on efficiency droop in InGaN/GaN light-emitting diodes based on differential carrier lifetime analysis,” *Applied Physics Letters,* vol. 108, no. 1, pp. 013501, 2016.

[28] M. F. Schubert, S. Chhajed, J. K. Kim, E. F. Schubert, D. D. Koleske, M. H. Crawford, S. R. Lee, A. J. Fischer, G. Thaler, and M. A. Banas, “Effect of dislocation density on efficiency droop in GaInN/GaN light-emitting diodes,” *Applied Physics Letters,* vol. 91, no. 23, pp. 231114, 2007.

[29] D. G. Kent, K. P. Lee, A. P. Zhang, B. Luo, M. E. Overberg, C. R. Abernathy, F. Ren, K. D. Mackenzie, S. J. Pearton, and Y. Nakagawa, "Effect of N2 plasma treatments on dry etch damage in n- and p-type GaN," *Solid-State Electronics,* vol. 45, no. 3, pp. 467-470, 3//, 2001.

[30] Q. Fan, S. Chevtchenko, X. Ni, S.-J. Cho, F. Yun, and H. Morkoç, "Reactive ion etch damage on GaN and its recovery," *Journal of Vacuum Science & Technology B: Microelectronics and Nanometer Structures Processing, Measurement, and Phenomena,* vol. 24, no. 3, pp. 1197-1201, 2006.

초 록

이 논문에서는 다중 양자 우물 구조 (MQW)를 가진 InGaN/GaN 기반의 발광다이오드의 efficiency droop 을 감소시키기 위한 직접 정공 주입 방식을 제안하고 연구하였다. 기존의 복잡하고 고비용의 nano-structure 공정 대신 간단한 방법을 통해 plug 모양의 정공 주입 구조 (DHIP)를 제작하고 그 특성을 여러 시뮬레이션과 소자제작을 통해 확인하였다. 시뮬레이션 에서는 DHIP 구조의 폭과 깊이를 조절하여 구조를 최적화 하고 정공 농도와 발광 재결합을 수치적으로 표현 함으로서 그 성능을 검증하였다. 그 결과 DHIP 는 MQW 에 주입되는 정공을 분산시키며 최종적으로 광출력을 100 A/cm^2 에서 11% 가량 증가시킬 수 있었다. 시뮬레이션 검증 결과를 바탕으로 c-plane 사파이어 기판 상에 DHIP 구조와 REF 구조의 LED 소자를 제작하였으며, DHIP 는 다중 양자 우물 구조에서 첫 번째 quantum well 까지 건식 식각하여 p-type GaN 을 regrowth 하였다. 그 결과 광출력이 100 A/cm^2 에서 최대 23.2%만큼 증가하는 것을

확인하였다. 광출력이 향상되는 결과의 원인을 세부적으로 분석하기 위해 EL transient decay characteristics 와 EL intensity distribution image 를 분석하였다. EL decay characteristics 의 이론적인 계산을 통해 내부 양자 효율을 관련 재결합 상수와 함께 추출하였다. 계산된 내부 양자 효율의 결과로 DHIP 구조가 광 재결합과 efficiency droop 을 크게 개선시키는 것을 확인하였다. DHIP 구조를 최적화 하기 위해서는 DHIP 의 총 둘레가 커지는 것에 따른 defect 증가를 고려 해야 하며 최적 DHIP 둘레는 75 mm 근처인 것을 확인하였다.

주요어: 발광다이오드, 정공 주입, 효율 드룹, 내부 양자효율, 질화갈륨 재성장, Light-emitting diodes (LEDs), hole injection, efficiency droop, internal quantum efficiency (IQE), lateral overgrowth (ELO)

학 번: 2015-20900